Int. J. Heat Mass Transfer. Vol. 29, No. 7, pp. 1051–1058, 1986
Printed in Great Britain

0017–9310/86 $3.00 + 0.00
Pergamon Journals Ltd.

Convection heat transfer from discrete heat sources in a rectangular channel

F. P. INCROPERA, J. S. KERBY, D. F. MOFFATT and S. RAMADHYANI
Heat Transfer Laboratory, School of Mechanical Engineering, Purdue University, West Lafayette, IN 47907, U.S.A.

(*Received* 22 *July* 1985 *and in final form* 15 *January* 1986)

Abstract—Experiments have been performed to determine convection heat transfer from a single heat source and an in-line, four-row array of 12 heat sources which are flush mounted to one wall of a horizontal, rectangular channel. The experiments were performed with water and FC-77 for channel Reynolds numbers ranging from approximately 1000 to 14,000. Results for a single heat source are in good agreement with those obtained for the first row of the array but exceed predictions based on conventional forced-convection correlations. The average convection coefficient for the rows of the array decreases by approximately 25% from the first to the second row and by less than 5% from the third to the fourth row. The data are in good agreement with model predictions for turbulent flow but are underpredicted for laminar flow.

INTRODUCTION

FEW SUBJECTS in heat transfer have been studied more extensively than that of internal forced convection. Numerous theoretical and experimental results have been obtained for laminar and turbulent flow in continuously heated ducts, and comprehensive reviews have been provided [1–4]. More recently, research has concentrated on means by which internal-flow heat transfer may be enhanced, as, for example, by using pins or ribs in a rectangular channel [5–8]. Despite such efforts, however, little attention has been given to the problem of forced-convection heat transfer from discrete sources attached to the walls of a duct. The problem is pertinent to the design and performance of strip heaters, as well as to the cooling of electronic circuits and the packaging of heat dissipating components.

Discrete heating at the walls of a duct may involve a single heat source (or multiple sources) embedded in a nonconducting (or conducting) substrate. For a flush-mounted heat source, thermal boundary-layer development may occur in the presence of a developing or a fully developed velocity profile, and for multiple sources, development of the thermal boundary layer is intermittent. If the heat source is mounted on a conducting substrate, thermal boundary-layer development may be influenced by preheating of the fluid due to conjugate wall effects, and if the source is small, heat transfer may be influenced by three-dimensional boundary-layer effects. This combination of conduction and advection edge effects may, in fact, preclude the applicability of conventional forced-convection correlations. Such effects have been noted by Baker [9], who found heat fluxes to be significantly underpredicted by conventional correlations for surface areas ranging from 200 to 1 mm^2.

The present study is primarily concerned with obtaining heat transfer data for square heat sources embedded in one wall of a rectangular duct, with emphasis placed on a single source and an in-line array of 12 sources which are flush mounted. Matters of particular interest concern the applicability of existing correlations to the isolated heat source, and the effect of intermittent thermal boundary-layer development on heat transfer from downstream rows of the array. Duct flow conditions range from laminar to turbulent ($1000 < Re_D < 14{,}000$), and experimental results are compared with numerical predictions based on a conjugate model for two-dimensional laminar and turbulent internal flow with discrete wall sources. The heat transfer fluids used in the study are water and FC-77 (a fluorocarbon liquid manufactured by 3M Company).

THEORETICAL PROCEDURES

In an effort to predict the experimental results of this study and to estimate substrate losses associated with specific heat source designs, a model was developed for conjugate conduction and forced convection heat transfer from small heat sources embedded in a large substrate. The system of interest (Fig. 1) involves one or more isothermal heat sources embedded in one wall of a horizontal channel, with hydrodynamically fully developed laminar or turbulent flow in the channel. The heat sources are flush mounted on a substrate material of thermal conductivity k_s and are insulated from the surroundings by a material of thermal conductivity k_i. With external system boundaries assumed to be adiabatic, all of the heat dissipated by the sources must be transferred by convection to the fluid, either directly from the sources or indirectly via the substrate. For simplicity, the heat sources are assumed to be strips of infinite length in the direction perpendicular to the paper, thus rendering the situation two-dimensional.

NOMENCLATURE

A_h	heat source surface area
D	channel hydraulic diameter
$\bar{h}$	average heat source convection coefficient
L_e	distance of first heat source from channel entrance
k	thermal conductivity
L_c	channel height
L_h	heat source length
L_o	overall channel length
L_s	heat source separation
$\overline{Nu}_L$	average heat source Nusselt number
P_h	heat source power dissipation
Pr	Prandtl number
Pr_t	turbulent Prandtl number
Re_D	Reynolds number based on duct hydraulic diameter
Re_L	Reynolds number based on heat source length
T	temperature
u	streamwise velocity
u_m	mean velocity
u^+	dimensionless velocity, u/v^*
v^*	friction velocity, $(\tau_w/\rho_f)^{1/2}$
x, y	longitudinal and cross-stream coordinates
W	channel width
y^+	dimensionless coordinate, yv^*/ν.

Greek symbols

α	thermal diffusivity
ε_M	turbulent diffusivity for momentum transfer
μ	dynamic viscosity
ν	kinematic viscosity
ρ	density
τ_w	wall shear stress.

Subscripts

f	fluid
h	heat source
i	heat source insulation
o	channel entrance condition;
s	substrate in which heat source is embedded.

Assuming steady, two-dimensional flow with constant thermophysical properties, the energy conservation equation for the fluid reduces to

$$u\frac{\partial T_f}{\partial x}=\left(\alpha_f+\frac{\varepsilon_M}{Pr_t}\right)\frac{\partial^2 T_f}{\partial x^2}+\alpha_f\frac{\partial^2 T_f}{\partial y^2}+\frac{\partial}{\partial y}\left(\frac{\varepsilon_M}{Pr_t}\frac{\partial T_f}{\partial y}\right) \tag{1}$$

where the turbulent diffusivity for momentum transfer is allowed to vary in the cross-stream direction. The $\partial^2 T_f/\partial x^2$ term is retained to render the equation elliptic, and the equation may be applied to laminar flow be setting $\varepsilon_M = 0$. With no advection in the substrate (and insulation), the appropriate form of the energy equation is

$$\frac{\partial^2 T_{s(i)}}{\partial x^2}+\frac{\partial^2 T_{s(i)}}{\partial y^2}=0. \tag{2}$$

Solutions to equations (1) and (2) are subject to the boundary conditions

$$T_f(0,y)=T_o \tag{3}$$

$$\left.\frac{\partial T_f}{\partial x}\right|_{x=L_o}=0 \tag{4}$$

$$\left.\frac{\partial T}{\partial n}\right|_{y\neq 0}=0 \tag{5}$$

where equation (3) prescribes a uniform temperature at the channel entrance, and equation (4) assumes the streamwise energy diffusion flux to be negligible at the outlet. With n representing the normal direction, equation (5) imposes an adiabatic condition at all substrate and insulation boundaries other than that for which $y = 0$. All interfacial contact resistances are neglected.

For laminar flow, the fully developed velocity profile is

$$\frac{u}{u_m}=6\left[\left(\frac{y}{L_c}\right)-\left(\frac{y}{L_c}\right)^2\right] \tag{6}$$

while for turbulent flow, it is approximated by the law of the wall [10]

$$u^+=y^+ \qquad (0\leqslant y^+<5) \tag{7a}$$

$$u^+=5.0+5.0\ln(y^+/5) \qquad (5\leqslant y^+<30) \tag{7b}$$

$$u^+=5.5+2.5\ln y^+ \qquad (30\leqslant y^+) \tag{7c}$$

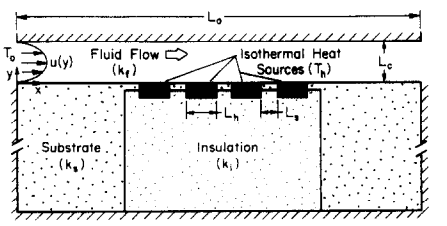

FIG. 1. Schematic of conjugate heat transfer model.

where $u^+ = u/v^*$ and $y^+ = yv^*/v$. The friction velocity, $v^* = (\tau_w/\rho)^{1/2}$, is related to the wall shear stress, which is evaluated from knowledge of the friction coefficient for fully developed, turbulent flow. The turbulent diffusivity is obtained from the Van Driest hypothesis [10]

$$\varepsilon_M = (0.4y)^2[1-\exp(-y^+/26)]^2|(\partial u/\partial y)| \quad (8)$$

where values of the Von Karman and Van Driest constants are taken to be 0.4 and 26, respectively. In the domain $0 \leqslant y \leqslant L_c/2$, equation (8) is used from $y = 0$ to that value of y for which ε_M reaches a maximum, and ε_M is fixed at the maximum value from that point to the midplane. A value of unity is assumed for the turbulent Prandtl number.

A control-volume, finite-difference procedure [11] was used to solve the governing equations, with the computation domain encompassing the fluid, substrate and insulation. Discontinuities in thermal conductivity, as, for example, at the substrate/fluid interface, were treated by placing a control surface at the interface and using the harmonic mean thermal conductivity. The procedure is consistent with the requirement of heat flux continuity at the interface.

The system of algebraic discretization equations obtained for the fluid and solid regions was solved through line-by-line application of the tri-diagonal matrix algorithm. The dimensions of the substrate were chosen to ensure a negligible influence of substrate size on the results. In particular, with the distance from the channel entrance to the first source, the distance from the last source to the channel exit, and the substrate thickness each equal to $7L_h$, solutions were found to be insensitive to further increases in the substrate dimensions. Validation of the numerical procedures was achieved through comparisons with existing exact solutions for unconjugated channel flows [12].

EXPERIMENTAL PROCEDURES

The heat source assembly used in the experiments of this study is shown schematically in Fig. 2. A chromium alloy resistance element is sputtered to a 12.7-mm-square, 1.59-mm-thick beryllium oxide substrate, and the substrate is joined to a 12.7-mm-square, 3.18-mm-thick copper block by a silver-filled epoxy. The surface temperature of the copper block is measured with a 5 mil copper–constantan thermocouple which is inserted from the side of the block and soft-soldered at the center of the surface. For studies involving a single heat source, a structural adhesive is used to mount and seal the source in a hole which is broached in a Lexan module ($k_s = 0.2$ W m^{-1} K^{-1}). A fine silica powder (Sylox 2) of low thermal conductivity ($k_i = 0.02$ W m^{-1} K^{-1}) is used to insulate the source from the surroundings. Similarly, for the heater array, which consists of four rows, with three heaters per row, the heaters are inserted in a Lexan module having

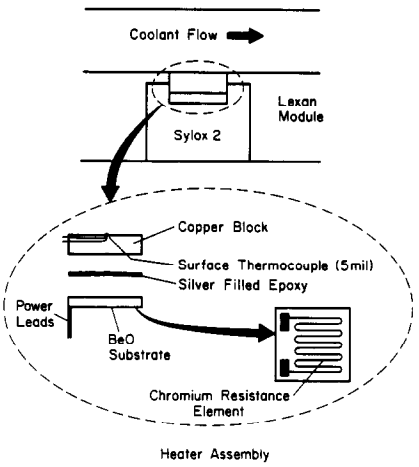

FIG. 2. Schematic of experimental heat source assembly.

12 broached holes, which are separated from each other by a distance of $L_s = 3.18$ mm. Silica powder is again used to insulate the heaters from the surroundings, and the assembly is mounted in the wall of the coolant channel.

Using the aforementioned conjugate analysis of thermal conditions in the channel flow, substrate and insulation losses for water were estimated to be less than 4.5% of the heater power for laminar flow and 2% for turbulent flow. Since such losses are within the experimental uncertainty of the measurements, they were neglected in reducing the data (all of the heater power was assumed to be transferred directly to the coolant). With FC-77 as coolant, the conjugate analysis revealed that heat transfer to the substrate may be as high as 12% in laminar flow and 8% in turbulent flow for a single heat source mounted in a Lexan substrate. Since these losses exceed the experimental uncertainties, corrections for substrate heat transfer have been applied to the data for the single heat source. However, since smaller substrate conduction effects were predicted for the array of four heat sources, the array data were not corrected.

From a separate analysis of heat source thermal conditions, it was found that temperature variations within the copper block were less than 0.1°C. Hence an average heat source convection coefficient may be based on a single temperature measurement for the copper block.

The flow channel to which the heater module is mounted is shown in Fig. 3. The experiments were performed in a rectangular duct of height $L_c = 11.9$ mm and width $W = 50.8$ mm, with the heat source located a distance of $L_e = 611$ mm from the flow straightener. The corresponding hydraulic diameter is $D = 19.3$ mm.

The flow channel is installed in a loop which includes a storage reservoir, pump, turbine flow meter, heat exchanger, and assorted valves and gages. The heat exchanger is used to dissipate heat added in the

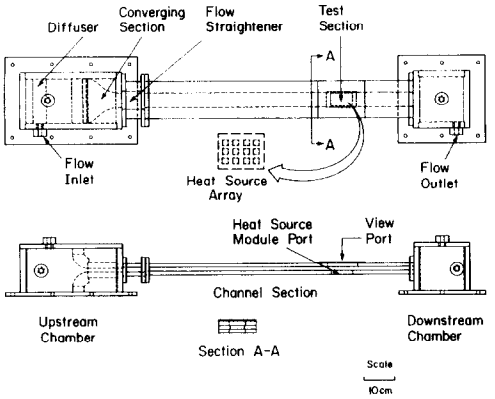

FIG. 3. Schematic of experimental flow channel.

test section and to regulate the temperature T_o of fluid entering the channel. An HP 3054 data acquisition system, under software control, continuously monitors the system temperatures and the electrical power to the heat source(s). The power circuit consists of a parallel network of heat sources, with a power rheostat and a current shunt placed in series with each source. The variable resistance of the rheostat allows for establishing the same power level or the same temperature in each heat source of the array, and the shunt is used to measure the current in each leg of the network. When the heat source temperatures reach steady state, the computer automatically reads and stores the temperature and power data for subsequent reduction.

Results for each heat source are presented in terms of an average Nusselt number which is defined as

$$\overline{Nu}_L = \frac{\bar{h}L_h}{k_o} = \frac{P_h L_h}{A_h(T_h - T_o)k_o} \tag{9}$$

where the heat source length is $L_h = 12.7$ mm and, for flush-mounted sources, the surface area is $A_h = 161\ \text{mm}^2$. All thermophysical properties are evaluated at the fluid inlet temperature, except for the viscosity μ_h, which is evaluated at the heater temperature and is used in the viscosity ratio, μ_o/μ_h, to account for nonconstant property effects.

Due to the unique geometry of the experimental system, two different characteristic lengths have been used to correlate the heat transfer data. Since the hydrodynamics correspond to internal channel flow, the hydraulic diameter D is used in calculating the Reynolds number. However, since thermal boundary-layer development is more closely associated with parallel flow over a plane surface, it is appropriate to base the Nusselt number on the heat source length. Hence the Nusselt number is defined as $\overline{Nu}_L = \bar{h}L_h/k_o$, while the Reynolds number is defined as $Re_D = u_m D/\nu$. Although it is uncommon to use different characteristic lengths in the same correlating equation, some justification is obtained from the energy equation. If L_h is used as a length scale in nondimensionalizing equation (1) and the Reynolds number is defined in terms of D, the ratio L_h/D emerges as a key parameter in the dimensionless form of the equation.

All experiments were performed in a horizontal channel with deionized water or FC-77, the fluids being thoroughly degassed prior to use. Measurements were made for fluid inlet temperatures of 14 and 30°C and Reynolds numbers in the range $1000 < Re_D < 14{,}000$. Dye injection studies revealed laminar and laminar/transitional flow characteristics for $Re_D < 4000$ and turbulent flow characteristics for larger Reynolds numbers. In all the experiments, the heat source-to-fluid temperature difference was maintained below 15°C in order to reduce nonconstant property effects. The experiments with the array of heat sources were run with uniform power input to the sources. Results of a detailed experimental uncertainty analysis [13] revealed uncertainties in $\overline{Nu}_L$ and Re_D to be less than 5%.

RESULTS

Experimental results obtained for a single, flush-mounted heat source, with water and FC-77, are plotted in Fig. 4 along with predictions based on the two-dimensional, numerical simulation. Thermophysical property values supplied by 3M Company have been used in reducing the FC-77 data. Two sets of symbols have been employed in plotting the FC-77 data: one set corresponds to data that has been corrected to account for substrate conduction effects, while the other set corresponds to the same data without correction for substrate heat transfer. The corrected FC-77 data and the water data are in excellent agreement with each other in the Reynolds number range $5000 < Re_D < 14{,}000$ and are correlated by the equation

$$\overline{Nu}_L = 0.13 Re_D^{0.64} Pr^{0.38} (\mu_o/\mu_h)^{0.25}. \tag{10}$$

The maximum deviations of the water and FC-77 data from the correlation are 4.9% and 5.8%, respectively.

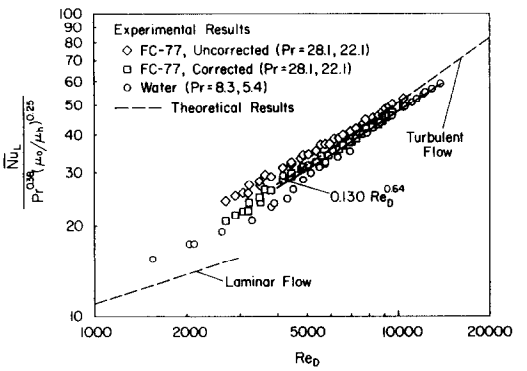

FIG. 4. Comparison of experimental and theoretical results for a square heat source of length $L_h = 12.7$ mm, flush-mounted in one wall of a rectangular channel of hydraulic diameter $D_h = 19.3$ mm.

In the range $3000 < Re_D < 5000$, the trend in the water results suggests a transition from laminar to turbulent flow. However, the FC-77 data do not exhibit such a trend. There is a noticeable, as yet unexplained, discrepancy between the two sets of data in this range.

The two-dimensional, theoretical predictions plotted on Fig. 4 are based on fluid thermophysical properties corresponding to those of water. These predictions differ from the experimental data for both water and FC-77 by a maximum of 7.2% and an average of 1.5% in the range $5000 < Re_D < 14{,}000$ (turbulent flow). For $Re_D < 3000$, the numerical results underpredict the data by approximately 30%, suggesting a breakdown in one or more of the model assumptions for laminar flow. Possibilities include failure to achieve fully developed conditions upstream of the heat source and/or the absence of two-dimensional, forced convection for flow over the source. With the reasonable proximity to fully developed flow which exists for $L_e/D = 25.7$ and the weak dependence of Nu on hydrodynamic entry region conditions for large Pr fluids [1], it is unlikely that the discrepancy may be attributed solely to hydrodynamic entry-region effects. The other possibilities include three-dimensional boundary-layer effects, which have been suggested as a mechanism for the enhancement of heat transfer from small sources [6], and/or the existence of mixed—rather than forced—convection. For turbulent flow, the heat source is positioned well beyond the hydrodynamic entry region, and the good agreement between the data and the predictions suggests that three-dimensional and mixed convection effects are negligible.

Having validated the two-dimensional, forced convection model for turbulent flow, parametric calculations were performed to extend the heat transfer results to conditions beyond those studied experimentally. Computations were performed for Reynolds numbers between 4000 and 10^6, Prandtl numbers of 0.7, 7 and 25, length scale ratios L_h/L_c of 0.1, 2 and 10, and thermal conductivity ratios k_s/k_f between 0.5 and 50. In these computations the presence of an insulation-filled cavity was not considered. That is, the substrate was assumed to be of uniform thermal conductivity k_s. The numerical predictions, which consist of 75 different cases involving the aforementioned parameter ranges, are correlated by an equation of the form

$$\overline{Nu}_L = 0.037 Re_D^{0.75} Pr^{0.35} (L_h/L_c)^{0.85} (k_f/k_s)^{0.02} \quad (11)$$

with a maximum deviation of $\pm 5\%$. For the smallest heat source length ($L_h/L_c = 0.1$), use of equation (11) is restricted to $Re_D > 100{,}000$ for $k_s/k_f < 10$ and $Re_D > 50{,}000$ for $k_s/k_f > 10$. Since this correlation encompasses much larger Reynolds numbers than the experimental correlation, equation (10), there is a stronger dependence of $\overline{Nu}_L$ on Re_D.

Attention was drawn earlier to the use of different length scales in the definitions of the Nusselt and Reynolds numbers. Equation (11) indicates that $\overline{Nu}_L$ depends strongly on (L_h/L_c) when the hydraulic diameter is employed in the definition of the Reynolds number. A much weaker dependence on (L_h/L_c) is indicated if the Reynolds number is defined in terms of the length of the heat source, L_h. The resulting correlation is

$$\overline{Nu}_L = 0.062 Re_L^{0.75} Pr^{0.35} (L_h/L_c)^{0.1} (k_f/k_s)^{0.02} \quad (12)$$

where $Re_L = u_m L_h/\nu$. This result suggests that, although hydrodynamic conditions correspond to those of internal flow, thermal conditions are more representative of external flow for the range of (L_h/L_c) examined in this study.

To test the applicability of conventional correlations to the system of interest, data for the single, flush-mounted heat source were compared with the Sieder–Tate correlation for fully developed, turbulent flow in a duct, $Nu_D = 0.027 Re_D^{4/5} Pr^{1/3} (\mu_o/\mu_h)^{0.14}$, and the correlation for the average Nusselt number associated with simultaneously developing, thermal and hydrodynamic turbulent boundary layers on a flat plate, $\overline{Nu}_L = 0.037 Re_L^{4/5} Pr^{1/3}$ [10, 14]. A more than 100% underprediction of the data by the Sieder–Tate correlation is attributed to the fact that the thermal boundary layer is far from fully developed over the length of the heat source and that conditions are more characteristic of a thermal entry region. Although still underpredicting the data, better agreement was achieved by the flat plate correlation. As shown in Fig. 5, agreement improves with increasing Reynolds number and is within approximately 15% at the high end of the Reynolds number range.

Experiments for the heat source array were performed with 12 flush-mounted heaters (four rows of three sources per row) at fluid inlet temperatures of 14 and 13°C. The same power was applied to each of the heaters, within the restriction that the temperature of heat sources in the last row not exceed the fluid inlet temperature by more than 15°C, in order to reduce nonconstant property effects. Since the water

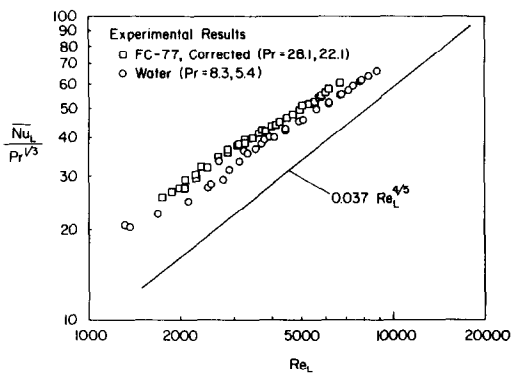

FIG. 5. Comparison of heat transfer data with correlation for turbulent flow over a flat plate.

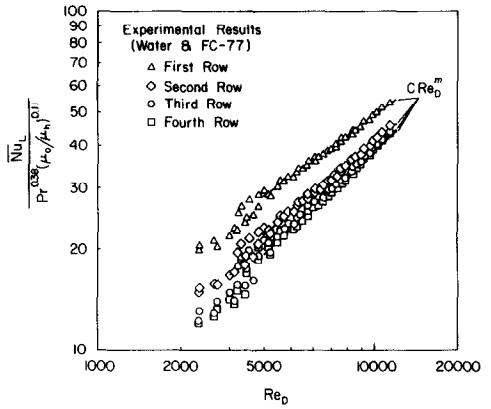

FIG. 6. Average Nusselt number for each row of the heat source array.

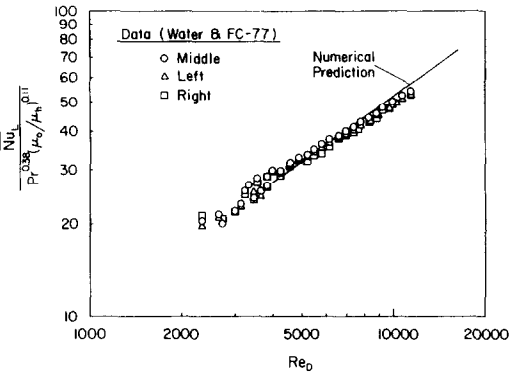

FIG. 7. Nusselt numbers for each heat source in the first row of the array and comparison with predictions for turbulent flow.

temperature never increased by more than 1.2°C across the array, the inlet temperature remained a convenient reference for evaluating the Nusselt number.

Average Nusselt numbers for the three heat sources of a row were computed, and the row-by-row variation is plotted in Fig. 6. A slight improvement in the extent to which the data may be collapsed was achieved by using a viscosity ratio exponent of 0.11 instead of 0.25. For each row, trends are consistent with those for the single heat source, but values for the first row are considerably larger than those for the last three rows. Results for the first row are 35% larger than those for the second row at small Reynolds numbers and 15% larger at the highest Reynolds number. Values of 15% and 5% are associated with a similar comparison of results for the second and third rows. Since there is little change in values between the third and fourth rows, it appears that a fully developed condition is achieved after the third row. The decrease in the percentage difference between the rows with increasing Reynolds number is attributed to diminished thermal boundary-layer growth across the upstream rows and hence a reduced effect of upstream sources on heat transfer from downstream sources.

As for the single heat source, empirical correlations were obtained for $Re_D > 5000$. The correlations are of the form

$$\frac{\overline{Nu}_L}{Pr^{0.38}(\mu_o/\mu_h)^{0.11}} = C\,Re_D^m \qquad (13)$$

where values of C and m are presented in Table 1 for each row of the array, along with maximum deviations of the data from the correlations. Percent deviations of the correlations from the data increase slightly with increasing row number. Heater-to-heater variations within a row are depicted for the first and fourth rows of the array in Figs. 7 and 8, respectively. Generally, the variations are small, the greatest scatter being observed in the range $3000 < Re_D < 4500$. Average and maximum variations for the first row are 3% and 8%, respectively; corresponding values for the fourth row are 5% and 10%, respectively. The largest Nusselt number is usually associated with the middle heater for both first and fourth rows, indicating that sidewall boundary layers are responsible for slightly diminishing the heat transfer rate from the two side heaters.

Average Nusselt numbers for the first row of the array, as well as Nusselt numbers for the middle source in the first row, are in good agreement with results obtained for the single heat source, although agreement is slightly better (within 5%) for the middle source. Once again, this result is attributed to the

Table 1. Constants of equation (13) for the array of 12 flush-mounted heat sources

	C	m	Maximum deviation (%)
Row 1	0.194	0.60	2.5
Row 2	0.069	0.69	2.7
Row 3	0.041	0.74	2.7
Row 4	0.029	0.78	3.9

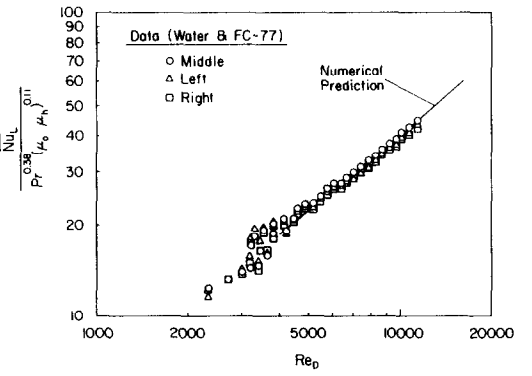

FIG. 8. Nusselt numbers for each heat source in the fourth row of the array and comparison with predictions for turbulent flow.

effect which sidewall boundary layers may have on reducing convection heat transfer from side heaters of the first row, thereby causing results for the single source to slightly exceed the average for the entire row. The excellent agreement between results for the single (isolated) heater and the middle heater suggests that three-dimensional substrate conduction effects are small. If such effects were significant, they should be diminished by the presence of the side heaters, which would act as guard heaters, thereby reducing heat transfer from the middle heater relative to that of the isolated heater.

Heat transfer data for the array are also compared with model predictions for turbulent flow in Figs. 7 and 8. The model simulates the three-dimensional array of 12 heat sources as a two-dimensional array of four heat sources. For each row, there is good agreement between the predictions and data for the Reynolds number range $5000 < Re_D < 12{,}000$. For the first row, the row average Nusselt number differs from the two-dimensional prediction by a maximum of 4%, while, for the fourth row, the difference is a maximum of 6%.

Although not shown, the row-by-row variation of the numerical predictions is similar to that obtained experimentally (Fig. 6). Numerical results for the first row are 25% larger than those for the second row for the lowest Reynolds number used in the calculations (4000) and 15% at the highest Reynolds number (15,000). Values of 9% and 5% are associated with a similar comparison of the numerical predictions for the second and third rows. The change in Nusselt numbers between the third and fourth rows is less than 3%. Thus, the row-by-row variation of the numerical results confirms that fully-developed conditions are reached after the third row.

SUMMARY

The problem of forced-convection heat transfer from discrete wall sources in a rectangular channel has been studied both experimentally and theoretically. Experimental results for a single flush-mounted heat source and an in-line, four-row array of 12 flush-mounted heat sources are correlated in terms of Nusselt and Reynolds numbers based on the source length and channel hydraulic diameter, respectively. Correlations have been obtained for the turbulent flow regime, $5000 < Re_D < 14{,}000$.

Model predictions are in good agreement with measurements for turbulent flow but significantly underpredict data for laminar flow. For turbulent flow, predictions and measurements for the array reveal approximately a 25%, 10% and 3% reduction in Nusselt numbers for successive rows from the first to the fourth. Based on comparisons between experimental results and predictions from the two-dimensional model, as well as between data for the isolated source and the first row of the array, it is concluded that three-dimensional substrate conduction and boundary-layer effects can be neglected for the conditions of this study. For the single heat source, numerical predictions of the Nusselt number have been correlated with Re_D, Pr, (L_h/L_c) and (k_s/k_f) over wide ranges of these parameters.

Although this study makes several contributions to the important problem of forced-convection heat transfer from distributed sources which are shrouded in a rectangular channel, it is clearly only a first step in resolving the effects of heat source size and spacing, channel hydraulic diameter and substrate conduction.

Acknowledgement–Support of this work by a grant from the IBM Corporation is gratefully acknowledged.

REFERENCES

1. R. K. Shah and A. L. London, *Laminar Forced Convection in Ducts, Advances in Heat Transfer, Supplement* 1. Academic Press, New York (1978).
2. B. S. Petukhov, Heat transfer and friction in turbulent pipe flow with variable physical properties. In *Advances in Heat Transfer* (Edited by T. F. Irvine and J. P. Hartnett), pp. 503–564. Academic Press, New York (1970).
3. W. M. Kays and H. C. Perkins, Forced convection, internal flow in ducts. In *Handbook of Heat Transfer* (Edited by W. M. Rohsenow and J. P. Hartnett), Chap. 7. McGraw-Hill, New York (1973).
4. B. S. Petukhov, A. F. Polyakov and O. G. Martynenko, Buoyancy effect on heat transfer in forced channel flows, *Proc. 7th Int. Heat Transfer Conference*, pp. 343–362. Hemisphere, New York (1982).
5. D. E. Metzger, R. A. Berry and J. P. Bronson, Developing heat transfer in rectangular ducts with staggered arrays of short pin fins, *J. Heat Transfer* **104,** 700–706 (1982).
6. R. J. Simoneau and G. J. Fossen, Jr., Effect of location in an array on heat transfer to a short cylinder in crossflow, *J. Heat Transfer* **106,** 42–48 (1984).
7. E. M. Sparrow, S. B. Vemuri and D. S. Kadle, Enhanced and local heat transfer, pressure drop, and flow visualization for arrays of block-like electronic components, *Int. J. Heat Mass Transfer* **26,** 686–699 (1983).
8. J. C. Han, J. S. Park and C. K. Lei, Heat transfer enhancement in channels with turbulence promoters, ASME Paper 84-WA/HT-72, Winter Annual Meeting, New Orleans (1984).
9. E. Baker, Liquid immersion cooling of microelectronic devices by free and forced convection, *Microelectron. Reliab.* **11,** 213–222 (1972).
10. L. C. Burmeister, *Convective Heat Transfer*. Wiley, New York (1983).
11. S. V. Patankar, *Numerical Heat Transfer and Fluid Flow*. Hemisphere/McGraw-Hill, New York (1980).
12. D. F. Moffatt, Convection heat transfer from discrete heat sources in the wall of a rectangular channel. MSME thesis, Purdue University, IN (1985).
13. S. J. Kline and F. A. McClintock, Describing uncertainties in single-sample experiments, *Mech. Engng* **75,** 3–8 (1953).
14. F. P. Incropera and D. P. DeWitt, *Fundamentals of Heat and Mass Transfer*. Wiley, New York (1985).

CONVECTION THERMIQUE A PARTIR DE SOURCES DISCRETES DE CHALEUR DANS UN CANAL RECTANGULAIRE

Résumé—Des expériences sont conduites pour déterminer le transfert thermique à partir d'une source unique de chaleur et à partir d'un arrangement en ligne de quatre rangées de douze sources de chaleur qui sont montées sur une paroi d'un canal horizontal et rectangulaire. Les expériences sont faites avec de l'eau et du FC 77, pour des nombres de Reynolds relatifs au canal allant approximativement de 1000 à 14000. Les résultats pour la source unique sont en bon accord avec ceux obtenus avec la première rangée mais dépassent les prévisions basées sur les formules conventionnelles de la convection forcée. Les coefficients moyens de convection pour les rangées décroissent approximativement de 25% de la première à la seconde rangée et de moins de 5% de la troisième à la quatrième. Les données sont en bon accord avec les prévisions pour l'écoulement turbulent mais pas pour l'écoulement laminaire.

KONVEKTIVER WÄRMETRANSPORT VON DISKRETEN WÄRMEQUELLEN IN RECHTECKIGEN STRÖMUNGSKANÄLEN

Zusammenfassung—Es wurden Versuche durchgeführt, um den konvektiven Wärmeübergang bei einer Anordnung zu beschreiben, welche aus einer einzelnen Wärmequelle und einer 4-reihigen Anordnung von 12 Wärmequellen besteht, die fluchtend an einer Wand eines waagerechten rechteckigen Strömungskanals montiert waren. Die Experimente wurden mit Wasser und FC-77 bei Reynolds-Zahlen von ungefähr 1000 bis 14000 durchgeführt. Die Ergebnisse für die einzelne Wärmequelle stimmen gut mit denen überein, die für die erste Reihe der mehrreihigen Anordnung ermittelt wurden. Sie übersteigen jedoch die aufgrund herkömmlicher Berechnungsmethoden für erzwungene Strömung zu erwartenden Ergebnisse. Der mittlere Wärmeübergangskoeffizient für die mehrreihige Anordnung nimmt ungefähr um 25% von der 1. zur 2. Reihe und um weniger als 5% von der 3. zur 4. Reihe ab. Die Versuchsergebnisse stimmen bei turbulenter Strömung gut mit den Modellberechnungen überein, werden jedoch bei laminarer Strömung zu klein berechnet.

КОНВЕКТИВНЫЙ ТЕПЛОПЕРЕНОС ОТ ДИСКРЕТНЫХ ИСТОЧНИКОВ ТЕПЛА В ПРЯМОУГОЛЬНОМ КАНАЛЕ

Аннотация—Проведены эксперименты по определению конвективного теплопереноса от одиночного источника тепла и от набора из 12 источников, расположенных в 4 параллельных ряда и вмонтированных заподлицо на одной стенке горизонтального прямоугольного канала. Эксперименты проводились с водой и FC-77 для чисел Рейнольдса в канале, изменяющихся от 1000 до 14000. Результаты для одиночного источника тепла хорошо согласуются с данными, полученными для первого ряда, но превышают расчетные, следующие из известных выражений для вынужденной конвекции. Осредненный коэффициент конвективного теплопереноса для рядов набора источников уменьшается приблизительно на 25% от первого до второго ряда и менее, чем на 5% от третьего до четвертого ряда. Данные хорошо соответствуют модельным расчетам для турбулентного потока, но занижены для ламинарного течения.